Thioether Binding of Low-Spin Bivalent Manganese. A MS_2N_4 Family Furnished by New Hexadentate Thioether-Oxime-Azo Ligands (M = Mn^{II}, Fe^{II}, Fe^{III})

Soma Karmakar, Suranjan Bhanja Choudhury, and Animesh Chakravorty*

Department of Inorganic Chemistry, Indian Association for the Cultivation of Science, Calcutta 700 032, India

Received June 3, 1994[⊗]

Four hexadentate ligands of type $HON{=}C(R)N{=}NC_6H_4S(CH_2)_xSC_6H_4N{=}NC(R){=}NOH$ (x = 2, 3; R = Ph, α-naphthyl) abbreviated as H_2RxL have been synthesized. These have afforded the low-spin complexes $Mn^{II}(RxL)$ (1.84-1.88 μ_B), $Fe^{II}(RxL)$(diamagnetic), and $[Fe^{III}(RxL)]ClO_4$ (1.92-2.10 μ_B). X-ray structure determination of Mn^{II}(Ph3L) has revealed the presence of a distorted octahedral MnS_2N_4 coordination sphere. The metal atom lies on a two-fold axis of symmetry. The Mn-N (1.900(12) Å, 1.923(10) Å) and the Mn-S (2.350(5) Å) lengths are much shorter than those in comparable thioether ligated high-spin manganese(II) species. Metal-ligand back-bonding is proposed to be present in Mn(Ph3L). Its magnetic moment decreases slightly with decreasing temperature as expected for the low-spin $3d^5$ configuration with substantially quenched orbital moment. In fluid solution, Mn(RxL) species exhibit six-line EPR spectra with a relatively low hyperfine constant (70-71 G). In frozen dichloromethane-toluene (77 K) solution anisotropic spectra are observed for both Mn(RxL) and Fe(RxL)$^+$. Oximato-N binding is an effective tool for inducing low-spin character. Crystal data for Mn(Ph3L) are the following: crystal system orthorhombic, space group *Pbna*, a = 8.753(5) Å, b = 14.575(7) Å, c = 21.297(12) Å, V = 2717(2) Å^3, Z = 4, R = 6.85%, R_w = 6.21%.

Introduction

This work forms part of our program on 3d-thioether coordination chemistry[1-4] and deals specifically with the case of manganese for which thioether ligated species are rare.[5-10] The first structural authentication of manganese(II)-thioether binding was recently achieved in a family of high-spin (s = $^5/_2$) complexes of coordination type $MnS_2N_2O_2$.[11] Herein we explore the feasibility of attaching low-spin (s = $^1/_2$) manganese(II) to the thioether function. There is no precedence of such binding and indeed low-spin manganese(II) is a generally uncommon entity.[12-16]

The above objective has been realized by designing a new family of acyclic hexadentate N,S ligands. The low-spin complexes are of coordination type $Mn^{II}S_2N_4$ and the X-ray structure of one member of the group has been determined. The isoelectronic $Fe^{III}S_2N_4$ species (and $Fe^{II}S_2N_4$ precursors) have also been prepared and characterized. Low-spin iron(III)-thioether chelates of acyclic N,S ligands have not been reported before.[17,18]

Results and Discussion

Ligand Design. The ligand system used in the present work is depicted in **1** and generally abbreviated as H_2RxL. It incorporates pairs of thioether, oxime, and azo functions correctly positioned for pseudooctahedral binding to a metal center. The four specific ligands used vary in R (Ph; α-naphthyl, Np) and/

[⊗] Abstract published in *Advance ACS Abstracts,* November 15, 1994.

(1) Choudhury, S. B.; Ray, D.; Chakravorty, A. *Inorg. Chem.* **1991**, *30*, 4354.
(2) Choudhury, S. B.; Ray, D.; Chakravorty, A. *J. Chem. Soc., Dalton Trans.* **1992**, 107.
(3) (a) Karmakar, S.; Choudhury, S. B.; Ray, D.; Chakravorty, A. *Polyhedron* **1993**, *12*, 291. (b) *Ibid.* **1993**, *12*, 2325. (c) Ray, D.; Pal, S.; Chakravorty, A. *Inorg. Chem.* **1986**, *25*, 2674.
(4) Chakraborty, P.; Karmakar, S.; Chandra, S. K.; Chakravorty, A. *Inorg. Chem.* **1994**, *33*, 816.
(5) Murray, S. G.; Hartley, F. R. *Chem. Rev.* **1981**, *81*, 365.
(6) Blake, A. J.; Schröder, M. *Adv. Inorg. Chem.* **1990**, *35*, 1.
(7) Cooper, S. R.; Rawle, S. C. *Struc. Bonding (Berlin)* **1990**, *72*, 1.
(8) Doedens, R. J.; Veal, J. T.; Little, R. G. *Inorg. Chem.* **1975**, *14*, 1138.
(9) Elias, H.; Schmidt, C.; Küppers, H.-J.; Wieghardt, K.; Nuber, B.; Weiss, J. *Inorg. Chem.* **1989**, *28*, 3021.
(10) Tomita, M.; Matsumota, N.; Agaki, H.; Okawa, H.; Kida, S. *J. Chem. Soc., Dalton Trans.* **1989**, 179.
(11) Chakraborty, P.; Chandra, S. K.; Chakravorty, A. *Inorg. Chem.* **1993**, *32*, 5349.
(12) Oxime complexes: (a) Chattopadhyay, S.; Basu, P.; Pal, S.; Chakravorty, A. *J. Chem. Soc., Dalton Trans.* **1990**, 3829. (b) Basu, P.; Pal, S.; Chakravorty, A. *Inorg. Chem.* **1988**, *27*, 1848. (c) Basu, P.; Chakravorty, A. *Inorg. Chem.* **1992**, *31*, 4980. (d) Basu, P.; Chakravorty, A. *J. Chem. Soc., Chem. Commun.* **1992**, 809. (e) Gouzerh, P.; Jeannin, Y.; Rocchiccioli-Deltcheff, C.; Valentini, F. *J. Coord. Chem.* **1979**, *9*, 221.
(13) Isothiosemicarbazide complexes: Knof, U.; Weyhermuller, T.; Wolter, T.; Wieghardt, K. *J. Chem. Soc., Chem. Commun.* **1993**, 726.
(14) Cyanides and cyanonitrosyl complexes: (a) Griffith, W. P. *Coord. Chem. Rev.* **1975**, *17*, 177. (b) Tullberg, A.; Vannerber, N.-G. *Acta Chem. Scand.* **1974**, *A28*, 551. (c) Monoharan, P. T.; Gray, H. B. *Chem. Commun.* **1965**, 324. (d) McNcil, D. A. C.; Raynor, J. B.; Symons, M. C. R. *J. Chem. Soc.* **1965**, 410. (e) Figgis, B. N. *Trans. Faraday Soc.* **1961**, *57*, 198. (f) *Ibid.* **1961**, *57*, 204. (g) Cotton, F. A.; Monchamp, R. R.; Henry, R. J. M.; Young, R. C. *J. Inorg. Nucl. Chem.* **1959**, *10*, 28.
(15) Isocyanide complexes: (a) Fantucci, P.; Naldini, L.; Cariati, F.; Valenti, V.; Bussetto, C. *J. Organomet. Chem.* **1974**, *64*, 109. (b) Matteson, D. S.; Bailey, R. A. *J. Am. Chem. Soc.* **1969**, *91*, 1975. (c) *Ibid.* **1967**, *89*, 6389. (d) Naldini, L. *Gazz. Chim. Ital.* **1960**, *90*, 871.
(16) Phosphine substituted carbonyls: (a) Connelly, N. G.; Hassard, K. A.; Dunne, B. J.; Orpen, A. G.; Raven, S. J.; Carriedo, G. A.; Riera, V. *J. Chem. Soc., Dalton Trans.* **1988**, 1623. (b) Carriedo, G. A.; Riera, V.; Connelly, N. G.; Raven, S. J. *J. Chem. Soc., Dalton Trans.* **1987**, 1769. (c) Bond, A. M.; Cotton, R.; McCormick, M. J. *Inorg. Chem.* **1977**, *16*, 155. (d) Stiddard, M. H. B.; Snow, M. R. *J. Chem. Soc.* **1966**, *A*, 777.
(17) Macrocyclic thioether complexes: (a) Blake, A. J.; Holder, A. J.; Hyde, T. I.; Schröder, M. *J. Chem. Soc., Chem. Commun.* **1989**, 1433. (b) Küppers, H.-J.; Weighardt, K.; Nuber, B.; Weiss, J.; Bill, E.; Trautwein, A. X. *Inorg. Chem.* **1987**, *26*, 3762.
(18) Porphyrin complexes with monodentate thioethers in axial positions: (a) McKnight, J.; Cheesman, M. R.; Reed, C. A.; Orosz, R. D.; Thomson, A. J. *J. Chem. Soc., Dalton Trans.* **1991**, 1887. (b) Cheesman, M. R.; Thomson, A. J.; Greenwood, C.; Moore, G. R.; Kadir, F. *Nature (London)* **1990**, *346*, 771. (c) Mashiko, T.; Reed, C. A.; Haller, K. J.; Kastner, M. E.; Scheidt, W. R. *J. Am. Chem. Soc.* **1981**, *103*, 5758.

0020-1669/94/1333-6148$04.50/0

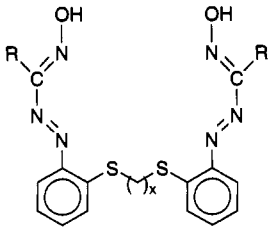

R	x	H_2RxL
Ph	2	H_2Ph2L
α-Naphthyl	2	H_2Np2L
Ph	3	H_2Ph3L
α-Naphthyl	3	H_2Np3L

1

or *x* (2; 3). The rationale behind the choice of **1** will now be briefly enumerated.

By itself the thioether function is a weak ligand for metal ions because of its poor σ-donor and π-acceptor character and its inability to neutralize cationic charge. For viable thioether coordination, ligands must have special stabilizing features. In the case of **1** these are multidenticity and anionic charge (oxime proton dissociation). In the crucial choice of companion sites that could promote spin-pairing we were guided by our recent experience that oximato-N coordination appears to induce low-spin character to manganese(II).[12] The azo moiety in **1** arose as part of the synthetic method used for incorporating the oxime group.

The essential steps involved in the synthesis of **1** are summarized in Scheme 1. Crucial among these is the reduction of the tetraazotized diamine to the dihydrazine hydrochloride **4**. This is best achieved using tin(II) chloride. The steps **4** → **5** → **1** were completed by extending the methods used for synthesis of bidentate azooximes.[19] The ligands were isolated as orange solids. To our knowledge **1** is the first organic system in which the thioether−oxime−azo triad of functions coexist.

The Complexes. The 1:1 reaction of H_2RxL with manganese(II) acetate tetrahydrate in methanol at room temperature afforded the brown colored Mn(RxL) complexes in excellent yields. The green iron(II) complexes, Fe(RxL), were similarly prepared from iron(II) perchlorate hexahydrate. The pink colored iron(III) family $[Fe(RxL)]ClO_4$ was best obtained in pure form by an electrochemical route: exhaustive one-electron oxidation of Fe(RxL) in dichloromethane solution at 1.0 V vs SCE.

In solution the bivalent complexes are nonelectrolytes and $[Fe(RxL)]ClO_4$ is a 1:1 electrolyte (Λ = 134−148 Ω^{-1} cm^{-1} M^{-1} in MeCN). All the complexes are electroactive in dichloromethane solution (Table 1, Figure 1). The one-electron $Fe(RxL)^+$−Fe(RxL) couple is observed as a nearly reversible cyclic voltammetric response with $E_{1/2}$, ~0.8 V. The manganese complexes also display a similar response ($E_{1/2}$, ~0.7 V) but the oxidized complex could not be isolated. Electronic spectral data of the complexes in the visible region in the dichloromethane solution are collected in Table 1 and representative spectra showing the distinctive features of the manganese(II), iron(II), and iron(III) families are displayed in Figure 1. The bands are too intense to be of ligand field origin.

Structure. The only complex that afforded single crystals is Mn(Ph3L). Even here the orthorhombic crystals were isolated as relatively weakly diffracting thin plates but a satisfactory structure could be worked out. Discrete molecules constitute the lattice. A view is shown in Figure 2 and bond parameters of the coordination sphere are listed in Table 2.

Scheme 1. (i) NaOMe in MeOH, $Br(CH_2)_xBr$, reflux; (ii) concentrated HCl, aqueous $NaNO_2$, stir at 0 °C; (iii) $SnCl_2$ in concentrated HCl, stir at 0 °C; (iv) aqueous NaOAC, glacial HOAC, RCHO, stir at 25 °C; (v) *n*-$BuNO_2$, NaOMe in MeOH, reflux; (vi) 4% aqueous NaOH at 25 °C for 12 h, extract with Et_2O, neutralize the aqueous part with 1 N H_2SO_4 at 0 °C.

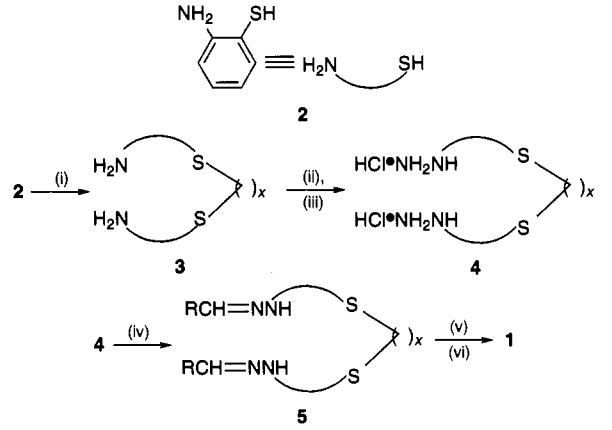

The ligand binds the metal in the hexadentate S_2N_4 fashion utilizing pairs of oximato-N, azo-N, and thioether-S atoms. The relative orientations within the pairs are cis, trans, and cis, respectively. The metal center as well as the middle dithiaalkylcarbon, C(15), lies on a crystallographic two-fold axis making the two meridional halves of the molecule equivalent.

The five-membered azooxime chelate ring, MnN_3C, is excellently planar with mean deviation of 0.02 Å. The thioether−azo chelate ring, $MnSNC_2$, is however mildly puckered, the mean deviation from the best plane being 0.07 Å. The six-membered dithiaalkyl ring, MnS_2C_3, has a skew-boat configuration (inset, Figure 2). The MnS_2N_4 coordination sphere is severely distorted from ideal octahedral geometry. The angles at the metal center between cis-positioned donor pairs span the range 78.8(5)−104.5(5) and those between trans-positioned pairs are 160.1(4) and 175.5(7).

The two Mn−S lengths, both 2.350(5) Å, in Mn(Ph3L) are equivalent by symmetry. The Mn−N(oxime) and Mn−N(azo) lengths are 1.900(12) and 1.923(10) Å, respectively. In the high-spin manganese(II) complexes **6** and **7**the average Mn−S (2.72

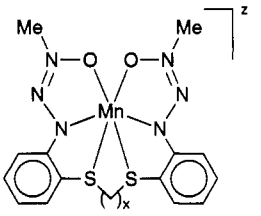

	z	x
6:	0	2
7:	0	3
6⁺:	+	2

Å) and Mn−N (2.14 Å) lengths[11] are much longer. Indeed these lengths in Mn(Ph3L) are even shorter than those in the high-spin manganese(III) complex $\mathbf{6}^+$ (Mn−S, 2.501(4) Å, Mn−N, 1.947(9) Å).[11]

A significant decrease in metal radius is anticipated upon spin-pairing.[20] The effect in Mn(Ph3L) is however very dramatic and the bond-lengths within the coordination sphere and the azo−oxime chelate rings suggests the presence of strong back-

(19) (a) Bamberger, E.; Pemsel, W. *Ber.* **1903**, *36*, 85. (b) Kalia, K. C.; Chakravorty, A. *J. Org. Chem.* **1970**, *35*, 2231.

(20) (a) Shannon, R. D. *Acta Crystallogr.* **1976**, *A32*, 751. (b) Shannon, R. D.; Prewitt, C. T. *Acta Crystallogr.* **1969**, *B25*, 925.

Table 1. Electrochemical[a] and Electronic Spectra Data in CH_2Cl_2 at 298 K

compounds	$E_{1/2}$,[b] V (ΔE_p,[c] mV); n[d,e]	UV-vis data, λ_{max}, nm (ϵ, M^{-1} cm^{-1})
Mn(Ph2L)	0.70 (100)	820 (1629), 725[f] (1628), 600 (2313), 490 (3877)
Mn(Ph3L)	0.71 (80)	800 (1738), 730[f] (1780), 590 (3646), 470 (7630)
Mn(Np2L)	0.72 (90)	810 (1740), 730[f] (1705), 600 (2436), 480 (4002)
Mn(Np3L)	0.69 (100)	800 (1818), 725[f] (1742), 600 (3560), 480 (7879)
Fe(Ph2L)	0.78 (90); (1.00)	850[f] (683), 700[f] (1079), 590 (2230), 460 (5395)
Fe(Ph3L)	0.80 (90); (1.02)	850[f] (651), 700[f] (1681), 610 (3526), 475 (6780)
Fe(Np2L)	0.79 (90); (1.01)	850[f] (629), 675[f] (1999), 610 (3407), 480 (6666)
Fe(Np3L)	0.78 (80); (1.00)	850[f] (634), 675[f] (1995), 610 (3506), 475 (6831)
[Fe(Ph2L)]ClO_4	0.78 (80); (0.99)	1000[f] (232), 725[f] (1272), 555 (5420), 480 (6305), 400[f] (7964)
[Fe(Ph3L)]ClO_4	0.79 (90); (1.00)	975[f] (305), 700[f] (1575), 550 (5984), 500 (5774), 400[f] (9238)
[Fe(Np2L)]ClO_4	0.79 (80); (0.98)	950[f] (271), 750[f] (1220), 550 (5593), 475 (6441)
[Fe(Np3L)]ClO_4	0.78 (80); (0.97)	950[f] (234), 725[f] (1269), 550 (6201), 480 (7324)

[a] At a platinum disk electrode; supporting electrolyte tetraethylammonium perchlorate (TEAP, 0.1 M); scan rate 50 mV s^{-1}; reference electrode SCE; solute concentration $\sim 10^{-3}$ M. [b] $E_{1/2}$ is calculated as the average of anodic (E_{pa}) and cathodic (E_{pc}) peak potentials. [c] $\Delta E_p = E_{pa} - E_{pc}$. [d] Constant-potential coulometric data $n = Q/Q'$, where Q is the observed coulomb count and Q' is the calculated count for 1e transfer. [e] Electrolysis performed at 200 mV above E_{pa} for oxidation and 200 mV below E_{pc} for reduction. [f] Shoulder.

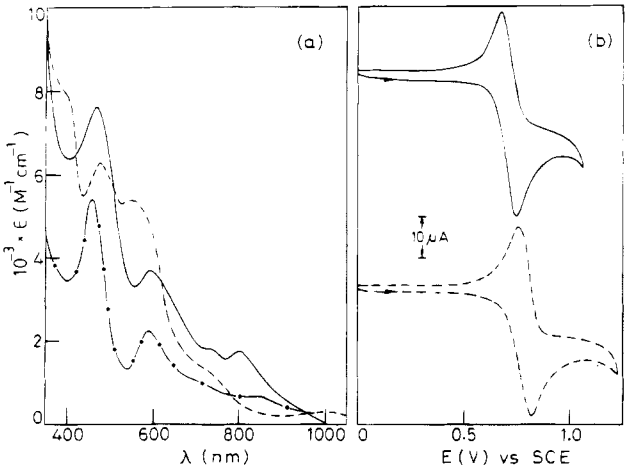

Figure 1. (a) Electronic spectra of Mn(Ph3L) (—), [Fe(Ph2L)]ClO_4 (- - - -) and Fe(Ph2L) (— • —) in dichloromethane. (b) Cyclic voltammograms (scan rate 50 mV s^{-1}) of 10^{-3} M solutions of Mn(Ph3L) (—) and Fe(Ph3L) (- - - -) in dichloromethane (0.1 M TEAP) at 298 K at platinum electrode.

Table 2. Selected Bond Distances (Å) and Angles (deg) and Their Estimated Standard Deviations for Mn(Ph3L)

	Distances		
Mn–S(1)	2.350(5)	N(2)–C(1)	1.329(17)
Mn–N(1)	1.900(12)	N(2)–N(3)	1.358(15)
Mn–N(3)	1.923(10)	N(3)–C(8)	1.394(17)
N(1)–C(1)	1.379(17)	C(13)–S(1)	1.762(14)
N(1)–O(1)	1.288(16)	C(14)–S(1)	1.842(17)
	Angles		
Mn–N(1)–C(1)	115.5(9)	N(1)–Mn–S(1A)	91.9(4)
Mn–N(1)–O(1)	124.0(9)	N(3)–Mn–N(1A)	104.5(5)
Mn–N(3)–C(8)	124.1(9)	N(3)–Mn–N(3A)	175.5(7)
Mn–N(3)–N(2)	118.2(8)	S(1)–Mn–N(1)	160.1(4)
Mn–S(1)–C(13)	97.8(5)	S(1)–Mn–N(3)	82.1(3)
Mn–S(1)–C(14)	109.0(6)	S(1)–Mn–N(3A)	94.8(3)
N(1)–Mn–N(1A)	87.2(7)	S(1)–Mn–S(1A)	95.5(2)
N(1)–Mn–N(3)	78.8(5)		

bonding (t_2(Mn)–π^* (azooxime) and d(S)). In effect there is a large contribution of a valence-bond situation like **8**. Structural

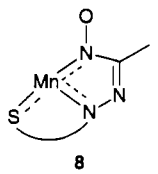

8

work on Ni^{II}(Ph3L) to be presented elsewhere has provided good indirect evidence in favor of this proposal.

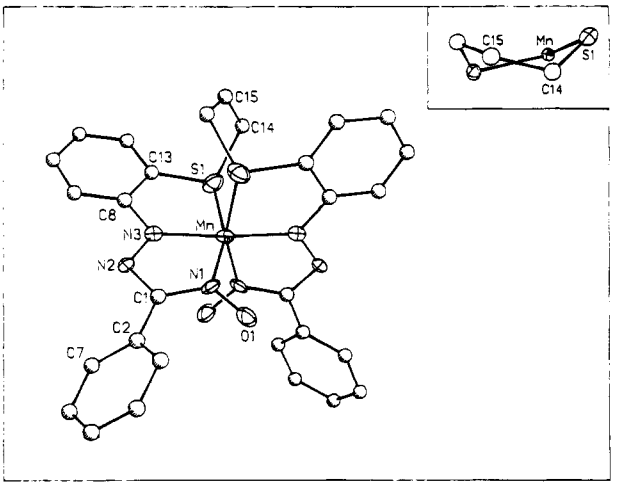

Figure 2. Perspective view and atom labeling scheme for Mn(Ph3L) with atoms other than carbon represented by their 30% probability ellipsoids. The MnS_2C_3 chelate ring is shown in the inset.

Table 3. Magnetic Moments[a] and EPR Data[b]

compounds	μ_{eff}, μ_B	g_{av}	A_{av}, G
Mn(Ph2L)	1.86	2.044	70.0
Mn(Ph3L)	1.88	2.045	70.8
Mn(Np2L)	1.84	2.043	71
Mn(Np3L)	1.86	2.044	70.2
[Fe(Ph2L)]ClO_4	2.03	2.081	–
[Fe(Ph3L)]ClO_4	1.92	2.079	–
[Fe(Np2L)]ClO_4	2.10	2.083	–
[Fe(Np3L)]ClO_4	2.07	2.086	–

[a] In the solid state at 298 K. [b] Dichloromethane–toluene (1:1) at 300 K.

Low-Spin Character. The room temperature (298 K) magnetic moments of solid Mn(RxL) and [Fe(RxL)]ClO_4 lie in the ranges 1.84–1.88 μ_B and 1.92–2.10 μ_B, respectively (Table 3). The Fe(RxL) complexes are diamagnetic. Thus all the species are low-spin: idealized t_2^5(Mn^{II},Fe^{III}) and t_2^6(Fe^{II}). The variable temperature moment of Mn(Ph3L) is displayed in Figure 3. The moment decreases slightly with decreasing temperature.

The moments of low-spin manganese(II) complexes are known to lie in the range 1.7–2.3 μ_B.[12–16] The decrease of the moment upon cooling is more pronounced in near-octahedral geometries where the orbital contribution is relatively high.[14e,f,16d] In Mn(Ph3L) there is substantial quenching of orbital moment, in qualitative agreement with the large distortions of the coordination sphere revealed by the X-ray work.

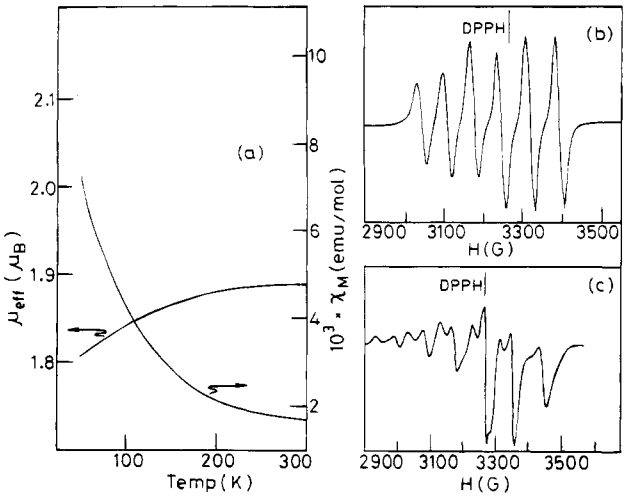

Figure 3. (a) Plots of the magnetic moment $\mu_{eff}(\mu_B)$ and the magnetic susceptibility χ_M (emu/mol) against temperature T (K) for Mn(Ph3L). (b) X-band EPR spectrum of Mn(Ph3L) in 1:1 dichloromethane–toluene solution at 300 K. (c) X-band EPR spectrum of Mn(Ph2L) in frozen 1:1 dichloromethane–toluene solution at 77 K.

In fluid solution the Mn(RxL) species exhibit six-line (^{55}Mn, $I = {}^5/_2$) EPR spectra (Figure 3). A notable feature is the relatively low value of the hyperfine coupling constant, A, 70–71 G (Table 3). In low-spin manganese(II) complexes A values span the range 75–100 G, the 90–100 G domain being more frequented.[14c,d,15a,16b–d] A decrease of A in Mn(RxL) is expected because of the Mn-ligand back-bonding.

In frozen (77 K) dichloromethane–toluene solution Mn(RxL) species display well-resolved anisotropic spectra. The representative case of Mn(Ph2L) is shown in Figure 3 ($g_1 = 2.061$, $A_1 = 102$ G; $g_2 = 2.036$, $A_2 = 96$ G; $g_3 = 2.009$, $A_3 \leq 15$ G). The Mn(RxL) spectra can be contrasted with those of high-spin **6** and **7** which show only very broad features spreading over the g regime 2–5 (zero-field splitting).[11] As in Mn(RxL), frozen solutions (77 K) of Fe(RxL)$^+$ exhibit well-resolved rhombic EPR spectra but without the complication of metal hyperfine structure. The g values of Fe(Ph3L)$^+$ are representative: $g_1 = 2.152$, $g_2 = 2.085$, $g_3 = 2.0018$.

Among bivalent 3d ions, manganese(II) has the highest spin-pairing energy[21] and only very strong-field ligands like CN$^-$, RNC, and CO (jointly with tertiary phosphines) induce low-spin character.[14–16] Of the donor sites present in H$_2$RxL, oximato-N can produce relatively large D_q values.[1,22] The present work taken collectively with our earlier findings[12] demonstrate that oximato-N coordination can indeed help in creating a ligand field strong enough to cause facile spin-pairing even in manganese(II). In Mn(RxL) the low-spin configuration is further consolidated by back-bonding. Finally, since Mn(RxL) is low-spin, Fe(RxL) and Fe(RxL)$^+$ must be so because of the general trends of spin-pairing energy ($Fe^{II} < Mn^{II} < Fe^{III}$) and D_q($Fe^{II} \sim Mn^{II} \ll Fe^{III}$).

Concluding Remarks. The main findings of this work will now be summarized. The binding of low-spin manganese(II) to the thioether function has been achieved for the first time via design of a hexadentate thioether–oxime–azo ligand systems, H$_2$RxL. The MnS$_2$N$_4$ coordination sphere in Mn(RxL) is distorted octahedral and the orbital magnetic moment is significantly quenched.

The Mn-ligand lengths in Mn(Ph3L) are appreciably shorter than those in comparable high-spin species (**6** and **7**). Low-spin character is supplemented by back-bonding with azooxime and thioether orbitals in causing the relatively large metal–ligand contractions. The ^{55}Mn EPR hyperfine coupling constants (~70 G) of Mn(RxL) are smaller than usual.

It is proposed that the strong σ-bonding of the oximato-N atoms plays a crucial role in inducing low-spin character in Mn(RxL) and other oximato complexes of bivalent manganese. It can be anticipated that H$_2$RxL would stabilize higher (>2) oxidation states of nickel and indeed it does so.

Experimental Section

Physical Measurements. A Hitachi 330 spectrophotometer was used to record UV-vis spectra. EPR spectra were studied with a Varian E-109C spectrometer fitted with a quartz dewar. Room temperature magnetic susceptibilities were measured with Model 155 PAR vibrating sample magnetometer fitted with a Walker Scientific L75FBAL magnet. Variable temperature data were collected with a George Associates Model 300 Lewis Coil force magnetometer. A Perkin-Elmer 240C elemental analyzer was used to collect microanalytical data (CHN). Electrochemical measurements were performed under nitrogen atmosphere on a PAR 370–4 electrochemistry system using solvents and supporting electrolyte purified/prepared as before.[23] The reference electrode was saturated calomel electrode (SCE). Solution electrical conductivities were measured with the help of a Philips PR 9500 bridge, the solute concentration being ~10^{-3} M.

Synthesis of Ligands and Complexes. The ligands were prepared by the same general procedure outlined in Scheme 1 and complexes were also synthesized by a general method. Details are given below for H$_2$Ph3L and its complexes. Analytical and some other data are provided for all ligands and complexes. The solvents and chemicals used for synthesis were of analytical grade.

1,3-Bis[(*o*-hydrazinophenyl)thio]propane Hydrochloride, 4 (R = Ph, *x* = 3). The diamine, 1,3-Bis[(*o*-aminophenyl)thio]propane, **3** (R = Ph, $x = 3$), was synthesized from 2-aminothiophenol following a literature method.[11,24] A solution of sodium nitrite (2.5 g, 0.036 mol) in 5 mL of water was added slowly to a suspension of the diamine (2.9 g, 0.01 mol) in 10 mL of concentrated HCl at 0 °C affording a clear greenish-yellow solution, which was left at 0 °C for a further period of 0.25 h. A cold solution (0 °C) of stannous chloride (12 g, 0.05 mol) in 10 mL of concentrated HCl was then added to it with vigorous stirring which was continued for 1.5 h. The yellow precipitate that separated was collected by filtration and then extracted with 30 mL of warm (60 °C) water to obtain a clear transparent solution which was cooled to room temperature and then 180 mL of concentrated HCl was added to it with constant stirring. The hydrazine hydrochloride **4** (R = Ph, $x = 3$) started separating immediately and the mixture was cooled overnight in a refrigerator. The crude white solid was collected by filtration and was used without further purification in the next step. Yield: 3.1 g (79%).

1,3-Bis[(*o*-(benzylidenehydrazo)phenyl)thio]propane, 5 (R = Ph, *x* = 3). A 3.1 g (0.0079 mol) amount of **4** (R = Ph, $x = 3$) was dissolved in a warm (50 °C) aqueous solution (15 mL) containing sodium acetate trihydrate (4.31 g, 0.03166 mol) and glacial acetic acid (10–15 mL). The solution was filtered to remove insoluble material, if any, and the filtrate brought to room temperature. To this, benzaldehyde (1.674 g, 0.0158 mol) was added slowly with vigorous stirring which was continued for 2 h. The pale yellow hydrazone separated immediately. It was collected by filtration and washed thoroughly with water and then dried in vacuo over fused CaCl$_2$ to obtain the required hydrazone, as a pale yellow solid. Yield: 3.5 g

(21) Lever, A. B. P. *Inorganic Electronic Spectroscopy*, 2nd ed.; Elsevier: New York, 1984; p 750.
(22) (a) Ray, D.; Chakravorty, A. *Inorg. Chem.* **1988**, *27*, 3292. (b) Chakravorty, A. *Isr. J. Chem.* **1985**, *25*, 99. (c) Nag, K.; Chakravorty, A. *Coord. Chem. Rev.* **1980**, *33*, 87. (d) Mohanty, J. G.; Chakravorty, A. *Inorg. Chem.* **1976**, *15*, 2912. (e) Mohanty, J. G.; Singh, R. P.; Chakravorty, A. *Inorg. Chem.* **1975**, *14*, 2178. (f) Drago, R. S.; Baucom, E. I. *Inorg. Chem.* **1972**, *11*, 2064. (g) E. I. Baucom, R. S. Drago, *J. Am. Chem. Soc.* **1971**, *93*, 6469.
(23) (a) Lahiri, G. K.; Bhattacharya, S.; Ghosh, B. K.; Chakravorty, A. *Inorg. Chem.* **1987**, *26*, 4324. (b) Basu, P.; Choudhury, S. B.; Pal, S.; Chakravorty, A. *Inorg. Chem.* **1989**, *28*, 2680.
(24) Unger, O. *Chem. Ber.* **1897**, *30*, 607.

(89.7%). Anal. Calcd for $C_{29}H_{28}N_4S_2$: C, 70.16; H, 5.64; N, 11.29. Found: C, 70.16; H, 5.66; N, 11.30. Mp: 92−94 °C.

Anal. Calcd for **5** (R = Ph, x = 2), $C_{28}H_{26}N_4S_2$: C, 69.71; H, 5.39; N, 11.62. Found: C, 69.72; H, 5.41; N, 11.63. Mp: 143−145 °C. Anal. Calcd for **5** (R = Np, x = 3), $C_{37}H_{32}N_4S_2$: C, 74.49; H, 5.37; N, 9.39. Found: C, 74.50; H, 5.35; H, 5.35; N, 9.40. Mp: 100−102 °C. Anal. Calcd for **5** (R = Np, x = 2), $C_{36}H_{30}N_4S_2$: C, 74.22; H, 5.15; N, 9.62. Found: C, 74.23; H, 5.13; N, 9.64. Mp: 150−152 °C.

1,3-Bis[*o*-[[α-(hydroxyimino)benzyl]azo]phenyl]thio]propane, 1 (R = Ph, x = 3). A 3.5 g (0.0070 mol) amount of **5** (R = Ph, x = 3) was suspended in 20 mL of dry methanol and 5 mL of freshly prepared *n*-$BuNO_2$ was added to the suspension followed by a solution of NaOMe in methanol (prepared from 0.7 g of Na in 15 mL of hot methanol). The blood red mixture was stirred and then heated to reflux for 1 h. It was cooled slowly in an ice-bath and then filtered. The filtrate was added to an ice-cold solution of 1 g of NaOH in 25 mL of water. The mixture was allowed to stand for 12 h at room temperature and then extracted with diethyl ether. The aqueous layer was cooled in ice and then neutralized slowly with cold 1 N H_2SO_4 until it became just acidic. During this process, the color of the solution became progressively lighter and finally the ligand, **1** (R = Ph, x = 3), separated out as a crystalline orange solid which was collected by filtration. It was washed several times with water and finally dried in vacuo over fused $CaCl_2$. Yield: 2 g (51%). Anal. Calcd for $C_{29}H_{26}N_6O_2S_2$: C, 62.81; H, 4.69; N, 15.16. Found: C, 62.80; H, 4.70; N, 15.15. Mp: 86−88 °C. UV-vis (CH_2Cl_2), λ_{max} in nm (ϵ in cm^{-1} M^{-1}): 400(sh), 325(15111).

Anal. Calcd for **1** (R = Ph, x = 2), $C_{28}H_{24}N_6O_2S_2$: C, 62.22; H, 4.44; N, 15.55. Found: C, 62.20; H, 4.46; N, 15.57. Mp: 128−130 °C. UV-vis (CH_2Cl_2), λ_{max} in nm (ϵ in cm^{-1} M^{-1}): 400(sh), 320(12677). Anal. Calcd for **1** (R = Np, x = 3), $C_{37}H_{30}N_6O_2S_2$: C, 67.89; H, 4.59; N, 12.84. Found: C, 67.87; H, 4.57; N, 12.83. Mp: 96−98 °C. UV-vis (CH_2Cl_2), λ_{max} in nm (ϵ in cm^{-1} M^{-1}): 410(sh), 310(11373). Anal. Calcd for **1** (R = Np, x = 2), $C_{36}H_{28}N_6O_2S_2$: C, 67.50; H, 4.37; N, 13.12. Found: C, 67.51; H, 4.35; N, 13.14. Mp: 132−134 °C. UV-vis (CH_2Cl_2), λ_{max} in nm (ϵ in cm^{-1} M^{-1}): 410(sh), 310(16115).

Propane-1,3-diylbis[α-[(*o*-thiophenylene)azo]benzaldoximato]-manganese(II), Mn(Ph3L). To a hot methanolic solution (15 mL) of H_2Ph3L (0.22 g, 0.4 mmol) was added a methanolic solution (5 mL) of manganese(II) acetate tetrahydrate (0.1 g, 0.4 mmol), and the mixture was stirred at room temperature for 0.5 h. The deposited dark crystalline solid was filtered off, washed with methanol, and dried in vacuo over P_4O_{10}. Yield: 0.20 g (83%). Anal. Calcd for $C_{29}H_{24}N_6O_2S_2Mn$: C, 57.33; H, 3.95; N, 13.84. Found: C, 57.32; H, 3.97; N, 13.84.

Anal. Calcd for Mn(Ph2L), $C_{28}H_{22}N_6O_2S_2Mn$: C, 56.66; H, 3.71; N, 14.17. Found: C, 56.66; H, 3.70; N, 14.18. Anal. Calcd for Mn(Np3L), $C_{37}H_{28}N_6O_2S_2Mn$: C, 62.81; H, 3.96; N, 11.88. Found: C, 62.83; H, 3.94; N, 11.88. Anal. Calcd for Mn(Np2L), $C_{36}H_{26}N_6O_2S_2Mn$: C, 62.34; H, 3.75; N, 12.12. Found: C, 62.34; H, 3.73; N, 12.11.

Propane-1,3-diylbis[α-[(*o*-thiophenylene)azo]benzaldoximato]-iron(II), Fe(Ph3L). To a hot methanolic solution (15 mL) of H_2Ph3L (0.15 g, 0.28 mmol) was added a methanolic solution (5 mL) of sodium acetate trihydrate (0.074 g, 0.54 mmol), and the mixture was stirred at room temperature for 0.25 h. A methanolic solution (10 mL) of $Fe(ClO_4)_2 \cdot 6H_2O$ (0.1 g, 0.276 mmol) was then added. Stirring was continued for a further period of 0.5 h. The deposited green solid was filtered off, washed with water and methanol and finally dried in vacuo over P_4O_{10}. Yield: 0.14 g (85%). Anal. Calcd for $C_{29}H_{24}N_6O_2S_2Fe$: C, 57.29; H, 3.95; N, 13.83. Found: C, 57.28; H, 3.93; N, 13.84.

Anal. Calcd for Fe(Ph2L), $C_{28}H_{22}N_6O_2S_2Fe$: C, 56.62; H, 3.71; N, 14.15. Found: C, 56.64; H, 3.70; N, 14.15. Anal. Calcd for Fe(Np3L), $C_{37}H_{28}N_6O_2S_2Fe$: C, 62.76; H, 3.96; N, 11.87. Found: C, 62.75; H, 3.94; N, 11.88. Anal. Calcd for Fe(Np2L), $C_{36}H_{26}N_6O_2S_2Fe$: C, 62.29; H, 3.75; N, 12.11. Found: C, 62.28; H, 3.76; N, 12.12.

Propane-1,3-diylbis[α-[(*o*-thiophenylene)azo]benzaldoximato]iron(III) Perchlorate, [Fe(Ph3L)]ClO_4. This complex was prepared electrochemically. Fe(Ph3L) (0.07 g, 0.115 mmol) was dissolved in 25 mL of dichloromethane and to it TEAP was added (0.026 g, 0.115 mmol). The green mixture was stirred at room temperature for 0.25 h and then subjected to exhaustive coulometric oxidation at 1.0 V vs SCE under nitrogen. The oxidation was stopped when the color of the solution became pink and the coulomb count corresponded to one-electron oxidation. The solution was filtered and the solvent then was evaporated under vacuo to obtain [Fe(Ph3L)]ClO_4 as a dark colored solid in pure form. Yield: 0.065 g (80%). Anal. Calcd for $C_{29}H_{24}N_6O_6S_2ClFe$: C, 49.23; H, 3.39; N, 11.88. Found: C, 49.22; H, 3.41; N, 11.88.

Anal. Calcd for [Fe(Ph2L)]ClO_4, $C_{28}H_{22}N_6O_6S_2ClFe$: C, 48.49; H, 3.17; N, 12.12. Found: C, 48.48; H, 3.15; N, 12.14. Anal. Calcd for [Fe(Np3L)]ClO_4, $C_{37}H_{28}N_6O_6S_2ClFe$: C, 55.02; H, 3.47; N, 10.41. Found: C, 55.00; H, 3.48; N, 10.40. Anal. Calcd for [Fe(Np2L)]ClO_4, $C_{36}H_{26}N_6O_6S_2ClFe$: C, 54.48; H, 3.28; N, 10.59. Found: C, 54.48; H, 3.26; N, 10.58.

Table 4. Crystallographic Data for Mn(Ph3L)

	Mn(Ph3L)		Mn(Ph3L)
chem formula	$C_{29}H_{24}N_6O_2S_2Mn$	T, °C	23
fw	607.6	λ, Å	0.71073
space group	*Pbna*	ϱ_{calcd}, g cm^{-3}	1.485
a, Å	8.753(5)	μ, cm^{-1}	6.79
b, Å	14.575(7)	R,[a] %	6.85
c, Å	21.297(12)	R_w,[b] %	6.21
V, Å^3	2717(2)	GOF[c]	1.43
Z	4		

[a] $R = \sum||F_o| - |F_c||/\sum|F_o|$. [b] $R_w = [\sum w(|F_o| - |F_c|)^2/\sum w|F_o|^2]^{1/2}$; $w^{-1} = \sigma^2(|F_o|) + g|F_o|^2$; g = 0.0003 for Mn(Ph3L). [c] The goodness of fit is defined as $[w(|F_o| - |F_c|)^2/(n_o - n_v)]^{1/2}$, where n_o and n_v denote the numbers of data and variables, respectively.

Table 5. Atomic Coordinates ($\times 10^4$) and Equivalent Isotropic[a] Displacement Coefficients (Å^2 $\times$ 10^3) for Mn(Ph3L)

	x	y	z	U(eq)
Mn	1734(3)	2500	0	25(1)
S(1)	−72(4)	1307(3)	18(3)	40(1)
O(1)	4183(11)	3764(7)	66(5)	47(4)
N(1)	3306(13)	3289(8)	−295(5)	28(4)
N(2)	2653(12)	2724(7)	−1265(5)	23(4)
N(3)	1647(13)	2275(7)	−889(5)	23(4)
C(1)	3591(15)	3250(10)	−931(6)	20(3)
C(2)	4840(17)	3716(10)	−1239(6)	30(4)
C(3)	5345(16)	4579(10)	−1063(7)	33(4)
C(4)	6599(17)	4971(11)	−1361(7)	39(4)
C(5)	7307(19)	4503(12)	−1826(8)	52(5)
C(6)	6875(19)	3658(11)	−2007(8)	59(5)
C(7)	5616(17)	3283(12)	−1719(6)	41(4)
C(8)	557(15)	1720(10)	−1178(6)	24(4)
C(9)	357(17)	1708(12)	−1834(7)	45(5)
C(10)	−776(19)	1165(11)	−2072(7)	51(5)
C(11)	−1752(22)	662(12)	−1695(8)	59(5)
C(12)	−1551(22)	685(12)	−1056(8)	58(5)
C(13)	−402(15)	1238(10)	−797(6)	29(4)
C(14)	−1887(19)	1750(12)	334(7)	63(5)
C(15)	−2653(28)	2500	0	85(8)

[a] Equivalent isotropic U defined as one-third of the trace of the orthogonalized U_{ij} tensor.

X-ray Structure Determination. Single crystals of Mn(Ph3L) were grown by slow evaporation from a 1:1 dichloromethane−toluene solution. A plate-like crystal of dimension 0.04 × 0.22 × 0.32 mm^3 was mounted on a glass fiber. The unit cell parameters were determined by the least-squares fit of 25 machine centered reflections having 2θ values in the range 15−25°. Systematic absences led to the identification of the space group as *Pbna*. Data were collected at 296 K by the ω-scan method over the 2θ range 2−51° on a Nicolet R3m/V diffractometer with graphite monochromated Mo Kα radiation (λ = 0.71073 Å). Two check reflections were measured after every 98 reflections during data collection to monitor crystal stability. No significant intensity reduction was observed in the 28 h of exposure to X-rays. All data were corrected for Lorentz-polarization effects. Empirical absorption correction could not be made due to unavailability of reflections of sufficient intensity in the required angular ranges. This however is not a serious limitation since the absorption coefficient is small (6.79 cm^{-1}). Of 2458 unique reflections 677 satisfying $I > 2.5\sigma(I)$ were used for structure solution. The structure was solved by direct

methods. The following non-hydrogen atoms were made anisotropic: Mn, all N, all O and S. Hydrogen atoms were added at calculated positions with $U = 0.08$ Å^2 in the last cycle of refinement. Significant crystal data are listed in Table 4. Atomic coordinates and isotropic thermal parameters are collected in Table 5. Computations were carried out on a Micro VAX II computer using the SHELXTL-PLUS program system[25] and crystal structure plots were drawn using ORTEP.[26]

(25) Sheldrick, G. M. SHELXTL-PLUS 88, *Structure Determination Software Programs*; Nicolet Instrument Corp.: 5225−2 Verona Road, Madison, WI 53711, 1988.
(26) C. K. Johnson, ORTEP, Report ORNL-5138, Oak Ridge National Laboratory, Oak Ridge, TN, 1976.

Acknowledgment. Crystallography was performed at the National Single Crystal Diffractometer Facility at the Department of Inorganic Chemistry, Indian Association for the Cultivation of Science. We are thankful to the Department of Science and Technology, New Delhi, for financial support. We also are indebted to Professor C. N. R. Rao and Dr. N. Vasanta Acharya for providing access to the Lewis coil magnetometer.

Supplementary Material Available: Tables of complete bond distances (Table S1) and angles (Table S2), anisotropic thermal parameters (Table S3), and hydrogen atom positional parameters (Table S4) for Mn(Ph3L) (3 pages). Ordering information is given on any current masthead page.